POLITECNICO DI TORINO
Repository ISTITUZIONALE

A Virtual Synchronous Machine Based Algorithm for Online Grid Impedance Estimation

Original
A Virtual Synchronous Machine Based Algorithm for Online Grid Impedance Estimation / Roveri, A., Mallemaci, V., Mandrile, F., Bojoi, R.. - (2024), pp. 740-747. (2024 IEEE Energy Conversion Congress and Exposition (ECCE) Phoenix, AZ, USA 20-24 October 2024) [10.1109/ecce55643.2024.10861752].

Availability:
This version is available at: 11583/2997466 since: 2025-02-11T17:17:37Z

Publisher:
IEEE

Published
DOI:10.1109/ecce55643.2024.10861752

Terms of use:

This article is made available under terms and conditions as specified in the corresponding bibliographic description in the repository

Publisher copyright
IEEE postprint/Author's Accepted Manuscript

©2024 IEEE. Personal use of this material is permitted. Permission from IEEE must be obtained for all other uses, in any current or future media, including reprinting/republishing this material for advertising or promotional purposes, creating new collecting works, for resale or lists, or reuse of any copyrighted component of this work in other works.

(Article begins on next page)

25 July 2026

A Virtual Synchronous Machine Based Algorithm for Online Grid Impedance Estimation

Alessandro Roveri
Prima Electro S.p.A.
Moncalieri (TO), Italy
alessandro.roveri@primaelectro.com

Vincenzo Mallemaci
Dipartimento Energia
Politecnico di Torino, Italy
vincenzo.mallemaci@polito.it

Fabio Mandrile
Dipartimento Energia
Politecnico di Torino, Italy
fabio.mandrile@polito.it

Radu Bojoi
Dipartimento Energia
Politecnico di Torino, Italy
radu.bojoi@polito.it

***Abstract*—In the growing context of integrating renewable sources and storage system in the electric grid, the virtual synchronous machine (VSM) concept represents a valid solution to embed grid support functionalities in grid-tied converters. The knowledge of grid impedance is required to exploit properly the VSM features in providing grid ancillary services, such as inertial behavior, harmonics compensation, as well as short circuit current injection during faults. Therefore, this paper proposes a closed-loop grid impedance estimator that is integrated into the VSM algorithm. The grid resistance and grid inductance estimations are performed in real-time, thus avoiding the data post-analysis that is usually required by methods available in the literature. The proposed solution leverages the VSM dependency on grid parameters when an amount of power is directly injected into the grid, without being processed by the VSM itself. The proposed estimator inherently rejects the noise on voltage and current measurements, thus providing reliable results for converter real world operating conditions affected by disturbances. Experimental tests on a 15 kVA grid-tied inverter are provided to validate the proposed solution.**

***Index Terms*—Grid impedance estimation, closed-loop integral estimator, virtual synchronous machines (VSMs), grid support, grid-connected inverters.**

I. Introduction

In the recent years, the integration of renewable energy sources into the grid is increasing worldwide, challenging the power system correct operation. Indeed, the grid stability must be guaranteed even in electrical systems with low inertia, where most of the power is provided by renewable power generators interfaced to the grid through static converters. The implementation of virtual synchronous machine (VSM) algorithms into the inverter control is a well-known solution to make the static converter behave as a traditional synchronous generator (SG), thus performing grid support and contributing to the power system stability [1-2]. Indeed, a VSM-driven inverter is enabled to provide the key ancillary services normally in charge of SGs, such as primary frequency and voltage regulation, inertial behavior, reactive support during faults, harmonic compensation and islanding capabilities [3].

As well as for SGs, the VSM operation is influenced by the grid impedance, which affects the power transfer capability and the local stability [4]. Therefore, the knowledge of grid impedance is needed for proper tuning of the VSM main functional blocks that are depicted in Fig. 1. Indeed, the grid inductance impacts on the damping of the active power loop controller [5] and the dynamic response of the reactive control [6]. Moreover, VSMs exhibit a coupling between active and reactive power in resistive systems [7] and some of the decoupling solutions proposed in the literature require a correct grid resistance estimation to properly compensate for the line resistive behavior [8]. Finally, the grid impedance estimation is also useful to properly tune the inverter current control [9]. According to the above-mentioned reasons, an accurate grid impedance computation is needed to adapt VSM parameters during operation.

The online local impedance estimation through grid-tied inverters is a research topic covered exhaustively in the literature [10]. Conventional local grid impedance estimation techniques rely on injecting controlled perturbations into the grid with subsequent frequency domain analysis of voltage and current response. For instance, a sinusoidal interharmonic of 75 Hz is injected in [11], while the network is excited with the non-characteristic frequencies of 400 and 600 Hz in [12]. Instead, an impulsive disturbance is injected in [9,13-14], thus enabling the grid impedance estimation in a wide range of frequencies. While ensuring high accuracy, these methods imply heavy data processing based on discrete Fourier transform (DFT). Moreover, the grid harmonic distortion increases and the compliance with international standards can be affected [15]. Other techniques leverage a variation of the active-reactive power references to modify the operating point and extract information about the network parameters, which are computed with algebraic tools at the end of the process [16]. They require a limited network disruption and offer a trade-off between accuracy and simplicity in implementation. However, P-Q reference variations result in a load angle deviation, which implies a rotation of the (d,q) synchronous reference frame during estimation. Therefore, in case of (d,q) controlled power converters, the grid parameters computation is negatively affected and the results accuracy reduces. An estimation improvement is obtained by increasing the number of investigated operating points to limit the effects of load angle deviation, at the cost of additional execution time [17-18]. The method proposed in [19] estimates the grid impedance by exciting the resonances of LCL filters used for grid interfacing. However, such an approach can result safety critical due to resonance amplifications. Moreover, it can affect the operation of other locally connected loads and converters.

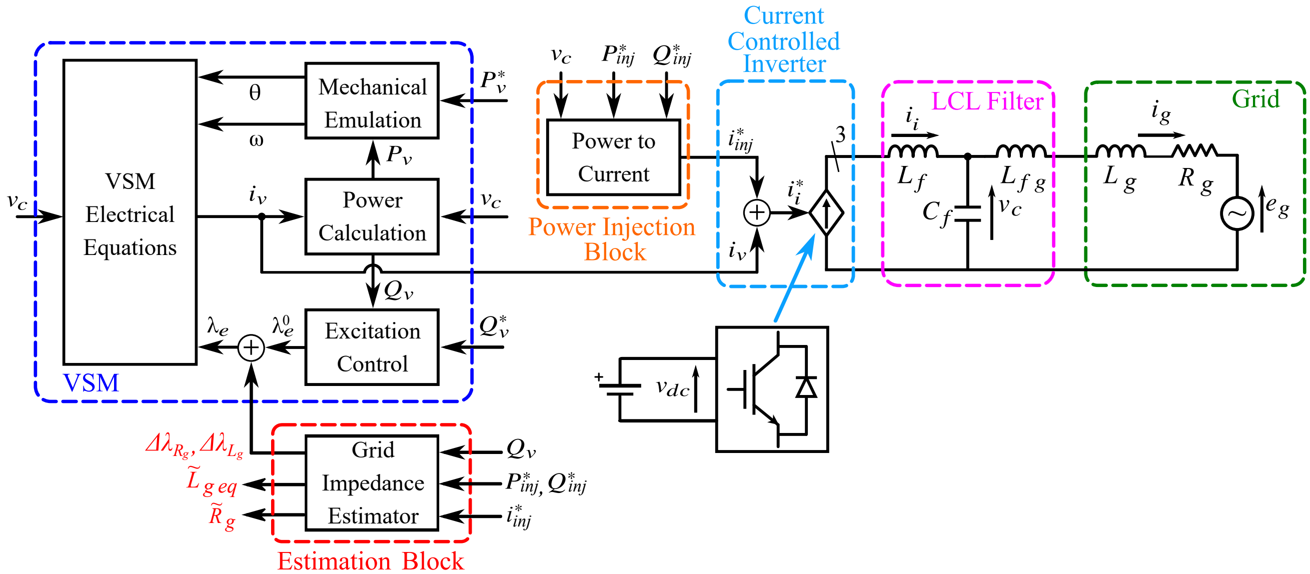

Fig. 1. VSM model embedded with the proposed grid impedance estimator (red highlighted). The VSM interfaces the grid and the integrated power injection block (orange highlighted) used for grid impedance estimation, which references are directly provided to the inverter current control.

Recent papers focused on the grid impedance estimation through grid-forming power converters [20-21]. A non-invasive technique is presented in [20]. However, the operation at zero active or reactive power reference is requested to estimate when the grid-tied inverter is power controlled. Furthermore, a Kalman filter is implemented to reject the noise and measurement errors, thus improving the estimation, while increasing the algorithm complexity and the computational effort. The method proposed in [21] requires only the active power variation to perform both the inductance and resistance estimation. Moreover, the phase error due to the load angle deviation during estimation is compensated and the method accuracy is improved. However, the grid impedance is computed through algebraic tools, thus resulting sensitive to the noise on current and voltage measurements. Although several algorithms are proposed in the literature to estimate the grid parameters through grid-tied power converters [9-21], no method directly exploits the VSM equations to perform a real-time grid impedance estimation. Consequently, the integration of additional algorithms into the inverter control is also needed in case of VSM-driven inverters, thus increasing the overall control algorithm complexity.

Therefore, this paper proposes a VSM-based closed-loop integral estimator, leveraging the VSM dependency on grid parameters when an amount of power is directly injected into the grid through the inverter current control, without being processed by the VSM (Power Injection Block in Fig. 1). The proposed method is implementable in any VSM with excitation control loop [1-2]. Compared to the solutions in the literature, the proposed algorithm does not require data post-processing, either with DFT or with algebraic calculations. In fact, the grid parameters are real-time estimated with reduced computational burden. Furthermore, the execution time is limited, since only a single power reference variation is requested to estimate the desired grid parameter. Moreover, the proposed integral estimator behaves as a low-pass filter, thus inherently rejecting the noise on current and voltage measurements and directly providing filtered results. Indeed, implementing improved filtering methods (i.e., Kalman filters) for better noise rejection is not needed, thus limiting the estimation computational effort. The estimator cut-off frequency and the procedure duration are settable by properly tuning the estimator integral gain. Finally, the proposed method requires a small amount of power injection ($\leq$ 0.1 pu) to obtain accurate results, with errors lower than 5%.

This paper is organized as follows. The functional blocks of the adopted VSM model are provided in Section II. Section III describes the linearized electrical model used to investigate the VSM dependence on grid parameters. Next, the proposed VSM-based closed-loop estimator is introduced in Section IV. Section V provides the experimental results on a 15 kVA setup. Section VI concludes the paper.

II. VSM Model

The block diagram of a current-controlled inverter with VSM control is depicted in Fig. 1. The VSM is embedded with the proposed grid impedance estimator and it interfaces the grid and the power injection block needed to add the external perturbation to perform the estimation. The VSM directly provides the current reference i_v to the inverter controller, thus injecting the desired active and reactive powers P_v-Q_v into the grid. Instead, the current i^*_{inj} is calculated from the external references P^*_{inj}, Q^*_{inj} and the voltage v_c, measured across the filter capacitor C_f. The current i^*_{inj} is directly injected into the grid through the inverter current control during the grid parameters estimation process. The VSM consists of the following functional blocks:

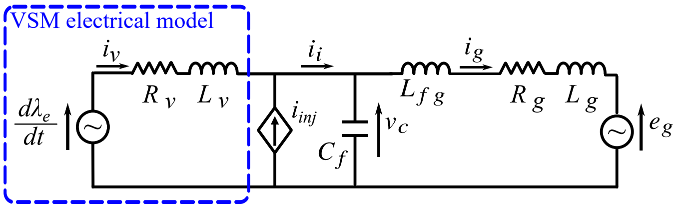

Fig. 2. Single phase electrical circuit of VSM interfaced to the grid and the injected current source.

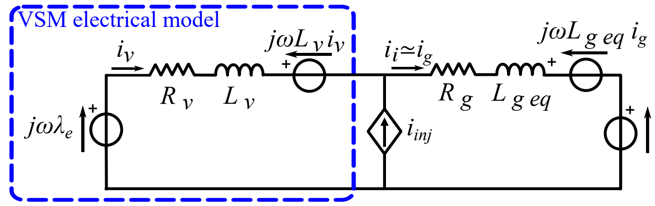

Fig. 3. Steady state equivalent circuit in the (d,q) reference frame rotating at ω. C_f is neglected and an equivalent $L_{g\ eq} = L_g + L_{fg}$ is considered.

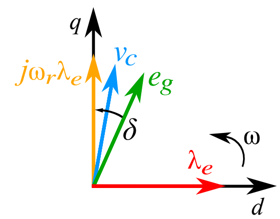

Fig. 4. Diagram of VSM excitation flux and grid voltage vectors in the (d,q) reference frame rotating at ω. δ is the load angle.

- *Power Calculation:* This function computes the VSM virtual active power P_v and reactive power Q_v by multiplying the virtual current i_v and v_c;
- *Mechanical emulation:* The block emulates the mechanical behavior of the VSM. It integrates the equation describing the motion dynamics of conventional SGs:

$$P_v^* - P_v = 2H\frac{d\omega}{dt} \tag{1}$$

  where P_v^* is the active power reference, H is the inertia constant and ω is the virtual rotor speed. Moreover, this block provides the orientation of the current controller θ;
- *Excitation control:* This feature regulates the VSM excitation flux λ_e^0 to provide the desired Q_v according to the reactive power reference Q_v^*. VSMs in the literature feature different reactive control solutions, such as models of the excitation winding of a real SG [22], droop-based proportional gain controllers [23], purely integral [24] or proportional-integral regulators [5];
- *Grid Impedance Estimator:* This block provides the grid impedance estimation. It computes the two terms $\Delta\lambda_{R_g}$ and $\Delta\lambda_{L_g}$, respectively added to λ_e^0 in case of grid resistance and inductance estimation. An exhaustive explanation of this block will be provided in Section IV;
- *Electrical Equations:* This function implements the virtual stator of the VSM. It provides the virtual current i_v, by receiving as inputs v_c, ω, θ and the resulting excitation flux λ_e.

The single phase equivalent circuit of Fig. 2 describes the interaction of the VSM with the grid and the injected current source. Since the inner current control loop is several order of magnitude faster than the VSM dynamic response, it is simplified as ideal, with a unity gain transfer function. Therefore, the inverter output current i_i is considered equal to the reference $i_i^* = i_v + i_{inj}^*$, as well as the injected current $i_{inj} \simeq i_{inj}^*$.

III. Linearized VSM Electrical Model

The steady state equivalent circuit in the (d,q) rotating reference frame is obtained by neglecting the derivative terms (Fig. 3). λ_e is aligned to the d-axis in the adopted (d,q) reference frame (Fig. 4). The grid inductance L_g and the grid-side LCL filter inductance L_{fg} can be merged in an equivalent series $L_{g\ eq}$. The steady-state electrical equation of the system in the q-axis is here reported:

$$\omega\lambda_e = R_v \cdot i_{v,q} + \omega L_v \cdot i_{v,d} + R_g \cdot i_{g,q} + \omega L_{g\ eq} \cdot i_{g,d} + e_{g,q} \tag{2}$$

where i_g is the grid current, e_g is the Thevenin equivalent grid voltage, while R_v, L_v, R_g and $L_{g\ eq}$ are the VSM and grid resistive and inductive elements. i_g can be substituted with $i_i = i_v + i_{inj}$, by neglecting the LCL filter capacitance C_f.

Therefore, assuming small variations around the operation point ($\omega \simeq 1$ pu), the per unit linearized equation in the q-axis is obtained as follows:

$$\begin{aligned}\Delta\lambda_e = (R_v + R_g)\cdot\Delta i_{v,q} + R_g\cdot\Delta i_{inj,q}\\ + (L_v + L_{g\ eq})\cdot\Delta i_{v,d} + L_{g\ eq}\cdot\Delta i_{inj,d} + \Delta e_{g,q}\end{aligned} \tag{3}$$

Eq. (3) demonstrates an interaction between the VSM and the injected current Δi_{inj}. Moreover, the active and reactive power exchange between the injected current source, the VSM and the grid can be expressed as:

$$P_{inj} = v_{c,q}\cdot i_{inj,q} + v_{c,d}\cdot i_{inj,d} \tag{4}$$

$$Q_{inj} = v_{c,q}\cdot i_{inj,d} - v_{c,d}\cdot i_{inj,q} \tag{5}$$

$$P_v = v_{c,q}\cdot i_{v,q} + v_{c,d}\cdot i_{v,d} \tag{6}$$

$$Q_v = v_{c,q}\cdot i_{v,d} - v_{c,d}\cdot i_{v,q} \tag{7}$$

Assuming the voltage v_c mainly aligned to the q-axis (Fig. 4), (4)-(7) are simplified as:

$$P_{inj} \simeq v_{c,q}\cdot i_{inj,q} \tag{8}$$

$$Q_{inj} \simeq v_{c,q}\cdot i_{inj,d} \tag{9}$$

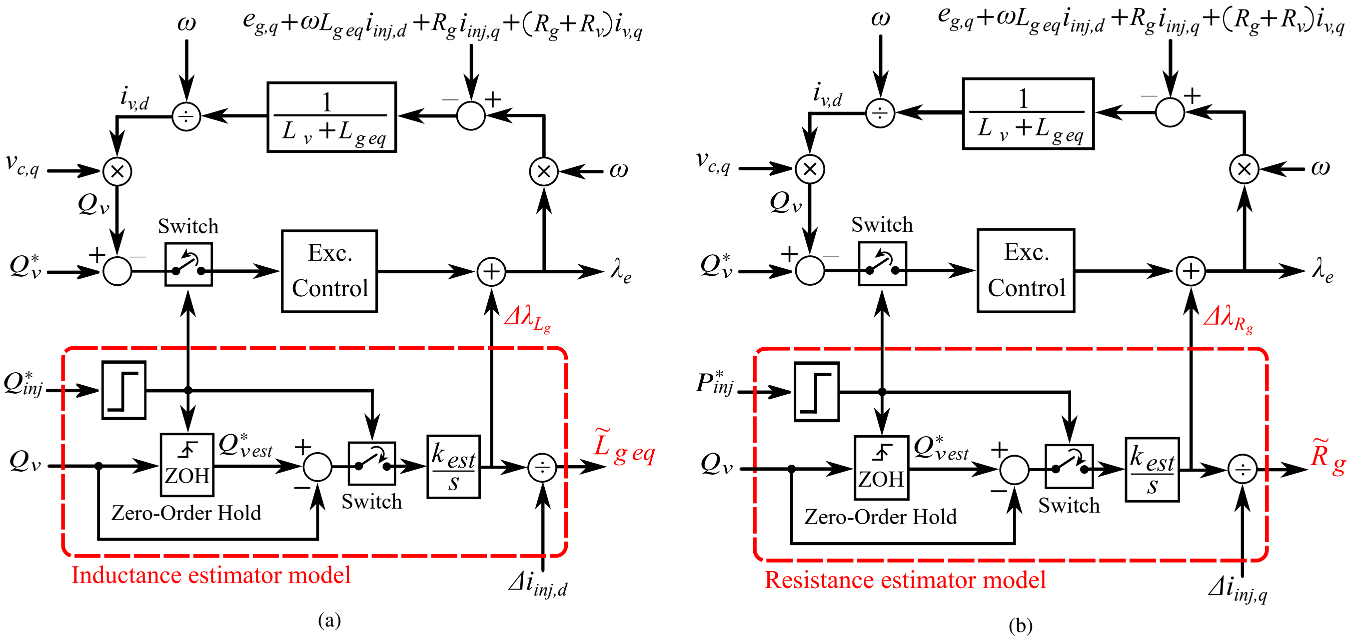

Fig. 5. Block diagram of the VSM excitation control integrating the proposed closed-loop estimator. The model is presented both in case of inductance (a) and resistance (b) estimation.

$$P_v \simeq v_{c,q} \cdot i_{v,q} \tag{10}$$

$$Q_v \simeq v_{c,q} \cdot i_{v,d} \tag{11}$$

According to (8), (9), $\Delta i_{inj,q}$ is obtained by varying the active power P_{inj}, while $\Delta i_{inj,d}$ by varying the reactive power Q_{inj}. When P_{inj} or Q_{inj} is injected into the grid, the mechanical emulation block limits the P_v perturbation (1). Consequently, according to (10), the deviation of $i_{v,q}$ in (3) is cancelled. Instead, $\Delta i_{v,d}$ can be compensated in (3) by adding to the excitation flux λ_e an extra term $\Delta\lambda_e$, dependent on grid parameters and proportional to the injected currents $\Delta i_{inj,d}$ and $\Delta i_{inj,q}$. Assuming constant grid voltage ($\Delta e_{g,q} \simeq 0$), the needed $\Delta\lambda_e$ to cancel $\Delta i_{v,d}$ is:

$$\Delta\lambda_e = R_g \cdot \Delta i_{inj,q} + L_{g\ eq} \cdot \Delta i_{inj,d} \tag{12}$$

Two different terms are derived from (12):

$$\Delta\lambda_{L_g} = L_{g\ eq} \cdot \Delta i_{inj,d} \tag{13}$$

$$\Delta\lambda_{R_g} = R_g \cdot \Delta i_{inj,q} \tag{14}$$

where $\Delta\lambda_{L_g}$ and $\Delta\lambda_{R_g}$ are the needed amounts of extra excitation flux to limit $\Delta i_{v,d}$ respectively in case of Q_{inj} and P_{inj} injection.

Therefore, a grid parameter estimator algorithm can be designed to take advantage of the grid parameters influences on the VSM reactive control loop, when an amount of active or reactive power is injected into the grid without being processed by the VSM itself.

IV. Proposed Estimation Method

The proposed closed-loop integral estimator algorithm is embedded into the VSM excitation control (Fig. 5). It can provide both the total grid inductance $\tilde{L}_{g\ eq}$ (Fig. 5a) and the grid resistance $\tilde{R}_g$ (Fig. 5b) according to which injected power reference is varied. Throughout the estimation procedure, the VSM power references P_v^*, Q_v^* are maintained constant.

Considering the q-axis electrical equation (2) and the simplified formula of reactive power (11), the excitation control feedback diagram of Fig. 5 is then obtained. When the injected power reference varies, the excitation control is disabled, while the estimator is triggered, taking over the task of regulating the reactive power. Moreover, the reactive power reference during estimation $Q_{v\ est}^*$ is set equal to the latest value of Q_v acquired before the estimation procedure is performed. Therefore, the desired Q_v, previously regulated by the excitation controller, is also guaranteed during the entire estimation process.

When Q_{inj} is injected, the integral estimator provides the additional excitation flux $\Delta\lambda_{L_g}$ needed to limit the Q_v-$i_{v,d}$ deviation. Then, $\tilde{L}_{g\ eq}$ is computed according to (13). Instead, $\Delta\lambda_{R_g}$ is calculated when a P_{inj} injection is performed. $\tilde{R}_g$ is thus obtained from (14). The tuning procedure is independent on the estimated grid parameter. The closed-loop estimator behaves as a low-pass filter and its characteristic equation is as follows:

$$s(L_v + L_{g\ eq}) + k_{est} \cdot v_{c,q} = 0 \tag{15}$$

where k_{est} is the estimator integral gain.

The system is thus governed by a single pole with the estimation time constant τ_{est} expressed as follows:

$$\tau_{est} = \frac{L_v + L_{g\ eq}}{k_{est} \cdot v_{c,q}} \tag{16}$$

The time constant τ_{est} is set to the desired value by properly tuning the closed-loop estimator gain k_{est}:

$$k_{est} = \frac{L_v + \tilde{L}_{g\ eq}}{\tau_{est} \cdot v_{c,q}} \tag{17}$$

Notably, the estimated grid inductance influences the k_{est} computation. Therefore, two different implementation strategies can be adopted: using the latest estimated value, or neglecting the inductance estimation term in the k_{est} computation (i.e., $\tilde{L}_{g\ eq} \simeq 0$) and accepting a slower response than the desired one. The real estimation time constant will be:

$$\tau_{est,real} = \frac{L_v + L_{g\ eq}}{L_v + \tilde{L}_{g\ eq}} \cdot \tau_{est} \tag{18}$$

As the other P/Q reference variation methods [10], [16-18], the proposed solution is based on the assumption that the grid voltage is constant during the estimation procedure ($\Delta e_{g,q} \simeq 0$). Indeed, the integral estimator is not able to discern whether $\Delta\lambda_e$ is due to external power injection or grid voltage deviation. The influence of $\Delta e_{g,q}$ on grid parameters computation is investigated by analyzing the transfer function $\frac{\Delta\lambda_e}{\Delta e_{g,q}}$:

$$\frac{\Delta\lambda_e}{\Delta e_{g,q}} = \frac{1}{\omega} \cdot \frac{k_{est} \cdot v_{c,q}}{s(L_v + L_{g\ eq}) + k_{est} \cdot v_{c,q}} \tag{19}$$

The grid parameter estimation error ΔZ_{err} due to $\Delta e_{g,q}$ is the same in case of grid inductance and resistance estimation. It can be computed by imposing $s \to 0$ (stationary response to step variation), assuming $\omega \simeq 1$ pu and dividing for the amount of injected current Δi_{inj}:

$$\begin{aligned} \left.\frac{\Delta Z_{err}}{\Delta e_{g,q}}\right|_{s\to 0} &= \frac{1}{\Delta i_{inj}} \cdot \left.\frac{\Delta\lambda_e}{\Delta e_{g,q}}\right|_{s\to 0} \\ &= \frac{1}{\Delta i_{inj}} \cdot \frac{1}{\omega} \simeq \frac{1}{\Delta i_{inj}} \end{aligned} \tag{20}$$

where $\Delta i_{inj} = \Delta i_{inj,d}$ in case of grid inductance estimation, while $\Delta i_{inj} = \Delta i_{inj,q}$ if the grid resistance is computed.

Therefore, the selected value of Δi_{inj} to perform estimation has to be small enough not to disturb the grid-tied converter operation, but sufficiently large to make the estimation insensitive to $\Delta e_{g,q}$. A value of $\Delta i_{inj} = 0.1$ pu is thus suggested. Moreover, a low estimation time constant τ_{est} reduces the execution time and consequently the risk of grid voltage deviation while performing the estimation. However, an improved noise rejection is obtained by increasing τ_{est}. A value of τ_{est} in the range of 50-100 ms is therefore chosen to perform experimental tests, thus limiting the duration of the procedure while guaranteeing filtered results.

Once the estimation process is completed, the integral estimator is disabled, while the VSM excitation controller is reactivated. Then, the new estimated values can be used to adapt online the gains of the VSM active [5] and reactive [6] power controllers, or to tune the inverter current regulators [9].

TABLE I
MAIN DATA OF THE EXPERIMENTAL SETUP

Base Values		**Inverter**		**VSM**		**Grid**	
S_b	15 kVA	S_n	15 kVA	L_v	0.1 pu	$L_{g\,eq}$	0.094 pu
V_b	210 V_{rms}	I_n	59 A	R_v	0.02 pu	R_g	0.107 pu
f_b	50 Hz	V_{dc}	380 V	H	4 s	L_{test}	0.033 pu
Z_b	2.9 Ω	f_{sw}	10 kHz	ζ	0.7	R_{test}	0.087 pu
		f_s	10 kHz	τ_{est}	50 - 100 ms		

V. EXPERIMENTAL RESULTS

The proposed closed-loop estimation algorithm has been embedded in the VSM model presented in [24]. The grid-tied converter is a 15kVA two-level three-phase inverter controlled by a dSPACE 1005 platform with 10 kHz of switching/sampling frequency. The inverter dc-link is supplied by a constant voltage source. The implemented reactive controller is a purely integral regulator. Meanwhile, the lead-lag damping solution of [25] is integrated in (1) with a desired damping coefficient $\zeta = 0.7$. Table I collects all the main data.

The VSM-controlled inverter is connected to a 50 Hz, 120 kVA, 210/400 V_{rms} line-line transformer through an LCL filter ($L_f = 545$ μH, $C_f = 22$ μF, $L_{fg} = 120$ μH), as illustrated in the scheme of Fig. 6. Moreover, a 300 μH inductor L_{test} and a 250 mΩ resistor R_{test} can be inserted in series with the LCL filter to online modify the grid inductance $L_{g\ eq}$ and resistance R_g.

To provide a benchmark for the proposed estimation method, the solution presented in [11] is implemented. Therefore, a non characteristic harmonic current of 75 Hz and 0.3 pu is injected into the grid to obtain an accurate grid impedance measurement. Then, current and voltage values are recorded and post-processed in MATLAB through Fast Fourier Transform (FFT). With L_{test} inserted and R_{test} shorted, the benchmark method computes a total grid inductance $L_{g\ eq,tot} = L_{g\ eq} + L_{test} = 0.127$ pu and a resistance $R_g = 0.107$ pu. Since L_{test} and R_{test} are known, $L_{g\ eq} = 0.094$ pu and $R_{g,tot} = R_g + R_{test} = 0.194$ pu are obtained. These results are used as expected values to compare with the proposed estimator method in experimental tests.

Two different tests validate the grid impedance estimation. In Test 1 (Fig. 7), the grid inductance and resistance are estimated with L_{test} inserted and R_{test} shorted, by injecting respectively $Q^*_{inj} = P^*_{inj} = 0.1$ pu and selecting $\tau_{est} = 50$ ms. The test is performed while the VSM is providing no power ($P^*_v = Q^*_v = 0$ pu). However, the proposed estimation algorithm can be executed with the VSM operating in any steady state condition. A non negligible ripple $\simeq 0.05$ pu is observed both on P_v and Q_v. These power deviations can be attributed to the noise on voltage measurements. Moreover, this noise is amplified due to the adopted voltage sensing solution. Indeed, only two phase voltages are measured, while

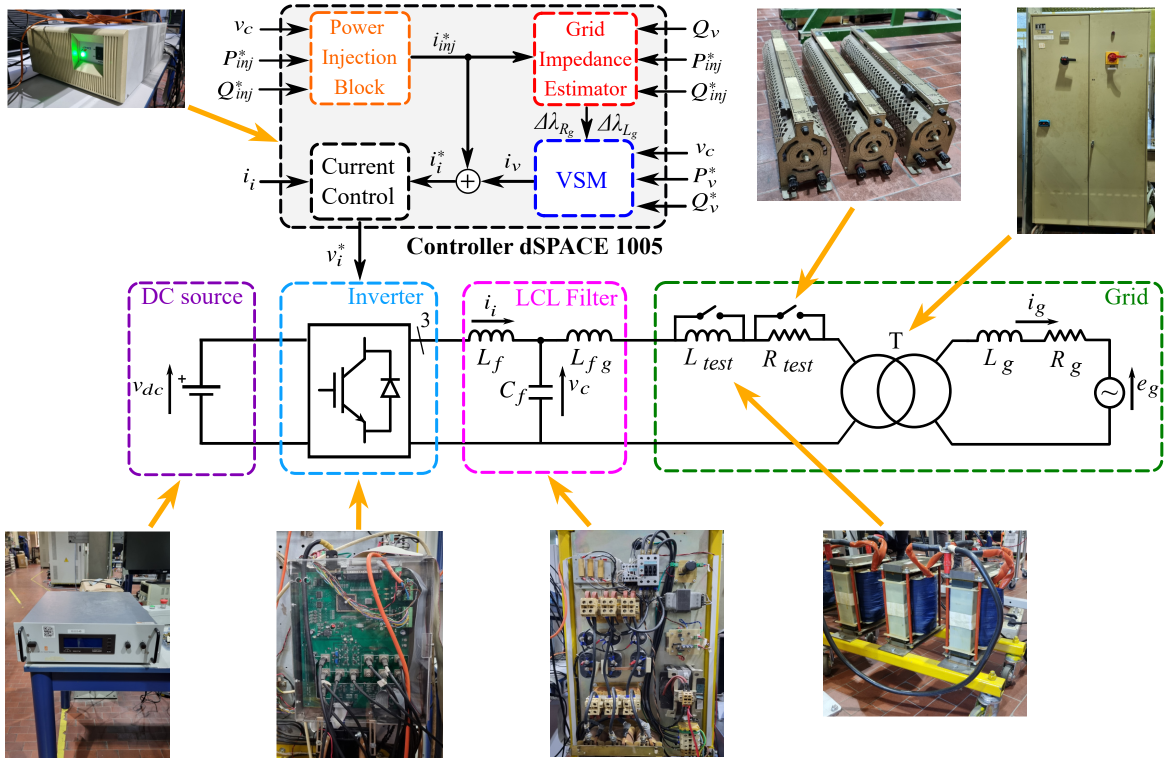

Fig. 6. Scheme and pictures of the hardware setup used for the experimental tests.

the third one is reconstructed. Fig. 7 also shows the moving-average filtered VSM power trends $P_{v\ filt}$-$Q_{v\ filt}$ to facilitate the insight of VSM operation during estimation.

The grid parameter estimation starts at $t = 0$ s, by setting the injected power reference to 0.1 pu. At the same time, the VSM excitation control is disabled, while the integral estimator takes charge of regulating the reactive power. Since the VSM is operating at zero reactive power before the estimation is performed, the estimator reactive power reference is $Q^*_{v\ est} = 0$ pu. According to the VSM linearized model described in (3), a non negligible Q_v is absorbed by the VSM due to the coupling with the Q^*_{inj}-P^*_{inj} power source. Then, the estimator provides the needed amount of excitation flux $\Delta\lambda_{L_g}$-$\Delta\lambda_{R_g}$ to cancel the Q_v deviation. k_{est} is computed by neglecting $\tilde{L}_{g\ eq}$. Therefore, according to (18), $\tau_{est,real} = 114$ ms results higher than τ_{est} by a factor of $\frac{L_v + L_{g\ eq}}{L_v} = 2.27$. The expected theoretical curves of estimated grid inductance and resistance during estimation process can be expressed as follows:

$$\tilde{L}_{g\ eq\ th} = L_{g\ eq} \cdot (1 - e^{-\frac{t}{\tau_{est,real}}}) \tag{21}$$

$$\tilde{R}_{g\ th} = R_g \cdot (1 - e^{-\frac{t}{\tau_{est,real}}}) \tag{22}$$

As it can be observed from Fig. 7, both the curves of $\tilde{L}_{g\ eq}$ and $\tilde{R}_{g\ eq}$ deviate from the theoretical values due to P_v fluctuations during grid parameters estimation. Indeed, the inverter is interfaced to a grid with a non negligible resistive behavior. Therefore, VSM features a coupling between active and reactive power [7] and when the reactive power varies, the active power changes as well. Moreover, the injection of P_{inj} results in a load angle deviation for VSM, which counteracts by absorbing active power. Although the mechanical emulation block operates to compensate for P_v variations and damp the oscillations during estimation, the active power control response affects the duration of the procedure. Therefore, the execution time may be limited by reducing the inertia constant H and adapting the damping coefficient ζ while performing grid impedance estimation. Despite the large ripple on virtual reactive power Q_v, the grid parameters estimation is accurate since the closed-loop integral estimator rejects the noise. Indeed, it behaves as a low-pass filter, whose cut-off frequency is as follows:

$$f_{cut-off\ est} = \frac{1}{2\pi \cdot \tau_{est,real}} = \frac{1}{2\pi \cdot 114 \text{ ms}} = 1.4 \text{ Hz} \tag{23}$$

Finally, the relative estimation errors of $\epsilon_{Lg} = -3.2\%$ and $\epsilon_{Rg} = -4.7\%$ are respectively obtained for grid inductance and resistance computation.

In Test 2 (Fig. 8), the impedance estimation method is performed while an external inductor L_{test} or resistor R_{test} is online inserted in series with the LCL filter. The estimation time constant τ_{est} is set to 100 ms. The $L_{g\ eq}$ computation in case of L_{test} insertion is shown in Fig. 8a. Before the test (i.e., $t < 0$ s), the injected power reference Q^*_{inj} is set to 0.1 pu, while the VSM excitation controller is disabled. At $t = 0$ s, the estimation algorithm is enabled and a first computation is performed. At $t \simeq 3.6$ s, L_{test} is inserted and the estimator, still enabled, immediately computes the new

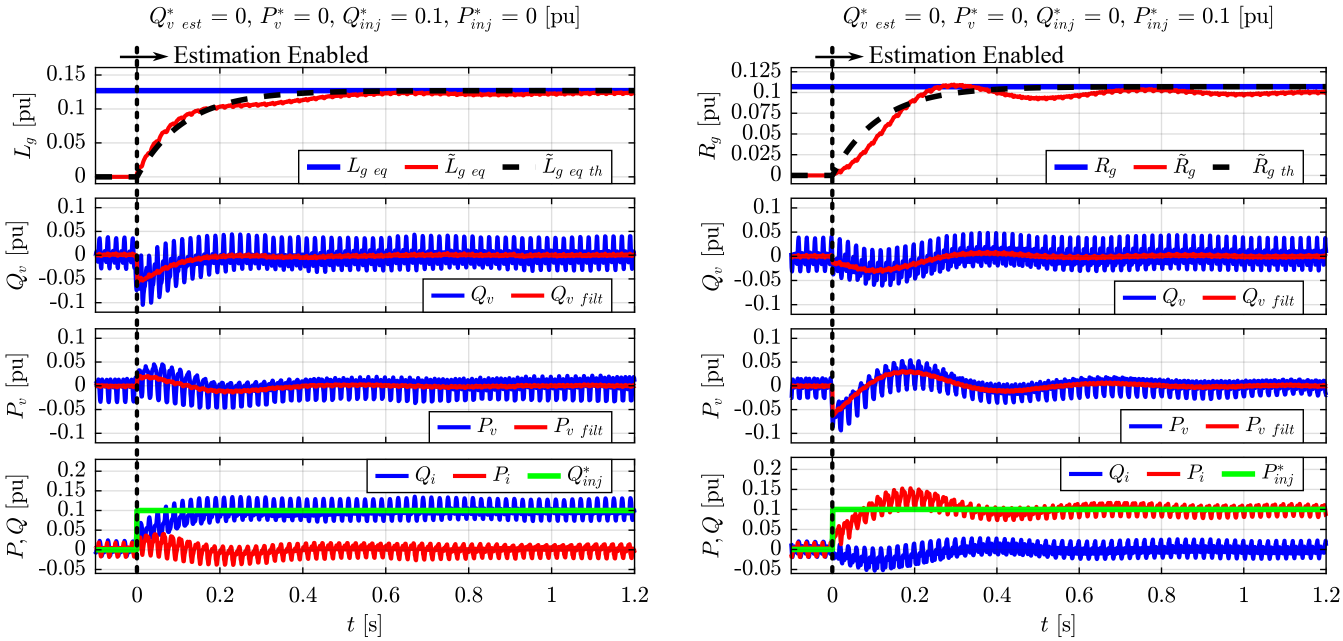

(a) (b)

Fig. 7. Results of Test 1: grid inductance (a) and resistance (b) estimation by respectively setting the external references $Q^*_{inj} = 0.1$ and $P^*_{inj} = 0.1$ pu. Meanwhile, the VSM operates at null power ($Q^*_{v,est} = P^*_v = 0$). From top to bottom: measured $L_{g\ eq}$-R_g, estimated $\tilde{L}_{g\ eq}$-$\tilde{R}_g$ and theoretical $\tilde{L}_{g\ eq\ th}$-$\tilde{R}_{g\ th}$ values of grid inductance and resistance; unfiltered Q_v and filtered $Q_{v\ filt}$ virtual reactive power; unfiltered P_v and filtered $P_{v\ filt}$ virtual active power; inverter output power Q_i-P_i and injected power references Q^*_{inj}-P^*_{inj}.

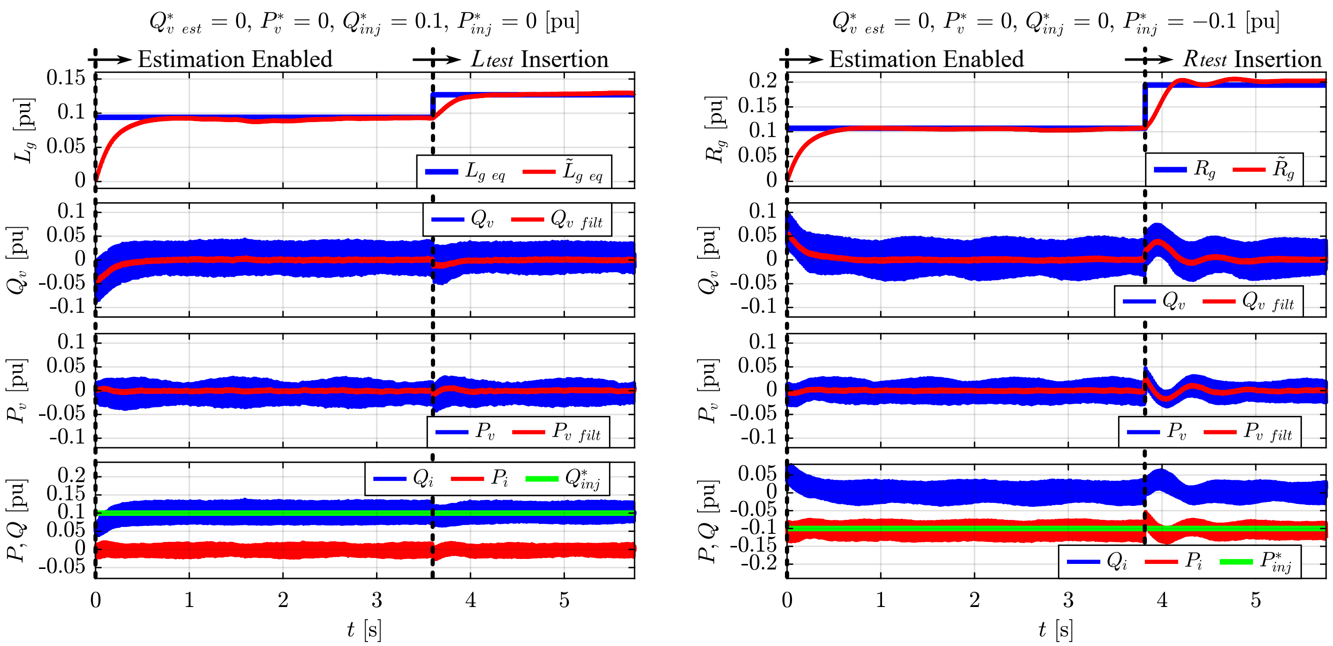

(a) (b)

Fig. 8. Results of Test 2: grid inductance (a) and resistance (b) estimation by respectively setting the external references $Q^*_{inj} = 0.1$ and $P^*_{inj} = -0.1$ pu. Meanwhile, the VSM operates at null power ($Q^*_{v,est} = P^*_v = 0$). From top to bottom: measured $L_{g\ eq}$-R_g and estimated $\tilde{L}_{g\ eq}$-$\tilde{R}_g$ values of grid inductance and resistance; unfiltered Q_v and filtered $Q_{v\ filt}$ virtual reactive power; unfiltered P_v and filtered $P_{v\ filt}$ virtual active power; inverter output power Q_i-P_i and injected power references Q^*_{inj}-P^*_{inj}.

inductance value. Accurate and filtered results are obtained without ($\epsilon_{Lg} = -1.1\%$) and with ($\epsilon_{Lg} = +1.6\%$) inserted L_{test}. The test is repeated to estimate R_g (Fig. 8b). P^*_{inj} is set to -0.1 pu to validate the proposed algorithm even in case of power absorption from the grid. The estimation process is enabled at $t = 0$ s, thus providing a first accurate

TABLE II
EXPERIMENTAL RESULTS OF GRID PARAMETERS ESTIMATION

	$L_{g\ eq}$ estimation			R_g estimation		
Test n°	Q^*_{inj} [pu]	$L_{g\ eq}$ [pu]	$\tilde{L}_{g\ eq}$ [pu]	P^*_{inj} [pu]	R_g [pu]	$\tilde{R}_g$ [pu]
Test 1	+0.1	0.127	0.123	+0.1	0.107	0.102
Test 2	+0.1	0.094	0.093	−0.1	0.107	0.108
	-	0.127	0.129	-	0.194	0.202

grid resistance computation ($\epsilon_{Rg} = +0.9\%$). The additional resistor R_{test} is inserted at $t \simeq 3.8$ s and the new value of estimated resistance is obtained with $\epsilon_{Rg} = +4.1\%$. The results of Test 1 and Test 2 are summarized in Table II, where the expected and the estimated values of $L_{g\ eq}$ and R_g are reported.

VI. CONCLUSION

This paper proposes a VSM-based closed-loop algorithm for estimating the equivalent grid inductance and grid resistance. The proposed method is an add-on feature integrated into the VSM excitation control loop, enabled when an amount of power not processed by VSM is directly injected into the grid through the inverter current control. A small external power injection ($\leq$ 0.1 pu) is needed to obtain accurate results. Therefore, the power system perturbation during the estimation process is limited. The estimation is performed in real-time, thus avoiding data post-processing through advanced mathematical tools (i.e., DFT), or with algebraic calculations. Moreover, the proposed estimator inherently rejects noise due to voltage and current measurement disturbances. Implementing advanced filtering solutions (i.e., Kalman filters) to improve the estimation accuracy is thus avoided. Therefore, the proposed algorithm results particularly suitable for field applications in disturbed environments. The estimator integral gain can be tuned according to the desired response time and the needed noise rejection capability. Indeed, the estimation duration can be reduced in less disturbed applications. Experimental tests have been carried out on a 15 kVA grid-tied inverter subjected to high noise on voltage measurements. The experimental results demonstrate the good accuracy and response time of the proposed estimation method, with errors below 5% and a response time in the range of 0.5 - 1 s.

REFERENCES

[1] V. Mallemaci, F. Mandrile, S. Rubino, A. Mazza, E. Carpaneto, and R. Bojoi, "A comprehensive comparison of virtual synchronous generators with focus on virtual inertia and frequency regulation," *Electric Power Syst. Res.*, vol. 201, p. 107516, 2021.

[2] M. Shadoul, R. Ahshan, R. S. AlAbri, A. Al-Badi, M. Albadi, and M. Jamil, "A comprehensive review on a virtual-synchronous generator: Topologies, control orders and techniques, energy storages, and applications," *Energies*, vol. 15, no. 22, 2022.

[3] "High penetration of power electronic interfaced power sources and the potential contribution of grid forming converters," ENTSO-E, Brussels, U.K., Tech. Rep., Jan. 2020.

[4] P. Kundur, *Power System Stability and Control.* McGraw-Hill Education, Jan. 1994.

[5] W. Zhang, A. Tarraso, J. Rocabert, A. Luna, J. I. Candela, and P. Rodriguez, "Frequency support properties of the synchronous power control for grid-connected converters," *IEEE Trans. Ind. Appl.*, vol. 55, no. 5, pp. 5178–5189, Sep. 2019.

[6] F. Mandrile, E. Carpaneto, E. Armando, and R. Bojoi, "Simple tuning method of virtual synchronous generators reactive control," *Proc. IEEE Energy Convers. Congr. Expo.*, pp. 2779–2785, 2020.

[7] M. Li, Y. Wang, W. Hu, S. Shu, P. Yu, Z. Zhang, and F. Blaabjerg, "Unified modeling and analysis of dynamic power coupling for grid-forming converters," *IEEE Trans. Power Electron.*, vol. 37, no. 2, pp. 2321–2337, Feb. 2022.

[8] A. Roveri, V. Mallemaci, F. Mandrile, and R. Bojoi, "Power decoupling method for grid inertial support provided by ultra-fast bidirectional chargers," *Proc. IEEE Energy Convers. Congr. Expo.*, pp. 6544–6546, 2023.

[9] M. Cespedes and J. Sun, "Adaptive control of grid-connected inverters based on online grid impedance measurements," *IEEE Trans. Sustain. Energy*, vol. 5, no. 2, pp. 516–523, 2014.

[10] M. K. De Meerendre, E. Prieto-Araujo, K. H. Ahmed, O. Gomis-Bellmunt, L. Xu, and A. Egea-Alvarez, "Review of local network impedance estimation techniques," *IEEE Access*, vol. 8, pp. 213 647–213 661, 2020.

[11] L. Asiminoaei, R. Teodorescu, F. Blaabjerg, and U. Borup, "Implementation and test of an online embedded grid impedance estimation technique for PV inverters," *IEEE Trans. Ind. Electron.*, vol. 52, no. 4, pp. 1136–1144, Aug. 2005.

[12] M. Ciobotaru, R. Teodorescu, and F. Blaabjerg, "On-line grid impedance estimation based on harmonic injection for grid-connected PV inverter," in *Proc. IEEE Int. Symp. Ind. Electron.*, 2007, pp. 2437–2442.

[13] M. Cespedes and J. Sun, "Online grid impedance identification for adaptive control of grid-connected inverters," *Proc. IEEE Energy Convers. Congr. Expo.*, pp. 914–921, 2012.

[14] P. Garcia, M. Sumner, A. Navarro-Rodriguez, J. M. Guerrero, and J. Garcia, "Observer-based pulsed signal injection for grid impedance estimation in three-phase systems," *IEEE Trans. Ind. Electron.*, vol. 65, no. 10, pp. 7888–7899, 2018.

[15] "IEEE recommended practice and requirements for harmonic control in electric power systems," *IEEE Std 519-2014 (Revision of IEEE Std 519-1992)*, pp. 1–29, 2014.

[16] A. V. Timbus, P. Rodriguez, R. Teodorescu, and M. Ciobotaru, "Line impedance estimation using active and reactive power variations," *Proc. IEEE Energy Convers. Congr. Expo.*, pp. 1273–1279, 2007.

[17] J.-H. Cho, K.-Y. Choi, Y.-W. Kim, and R.-Y. Kim, "A novel P-Q variations method using a decoupled injection of reference currents for a precise estimation of grid impedance," in *Proc. IEEE Energy Convers. Congr. Expo.*, 2014, pp. 5059–5064.

[18] N. Mohammed, T. Kerekes, and M. Ciobotaru, "An online event-based grid impedance estimation technique using grid-connected inverters," *IEEE Trans. Power Electron.*, vol. 36, no. 5, pp. 6106–6117, May 2021.

[19] M. Liserre, F. Blaabjerg, and R. Teodorescu, "Grid impedance estimation via excitation of LCL-filter resonance," *IEEE Trans. Ind. Appl.*, vol. 43, no. 5, pp. 1401–1407, Sep. 2007.

[20] J. Fang, H. Deng, and S. M. Goetz, "Grid impedance estimation through grid-forming power converters," *IEEE Trans. Power Electron.*, vol. 36, no. 2, pp. 2094–2104, 2021.

[21] J. Yu, W. Liu, J. Sun, F. Zhang, and Y. Yang, "An improved grid impedance estimator for grid-forming converters in consideration of controller dynamics," *Int. J. Electr. Power Energy Syst.*, vol. 154, p. 109424, 2023.

[22] H.-P. Beck and R. Hesse, "Virtual synchronous machine," in *Proc. 9th Int. Conf. Elect. Power Qual. Utilisation*, 2007, pp. 1–6.

[23] S. D'Arco, J. A. Suul, and O. B. Fosso, "A virtual synchronous machine implementation for distributed control of power converters in smartgrids," *Electric Power Syst. Res.*, vol. 122, pp. 180–197, 2015.

[24] F. Mandrile, E. Carpaneto, and R. Bojoi, "Grid-feeding inverter with simplified virtual synchronous compensator providing grid services and grid support," *IEEE Trans. Ind. Appl.*, vol. 57, no. 1, pp. 559–569, Jan. 2021.

[25] F. Mandrile, V. Mallemaci, E. Carpaneto, and R. Bojoi, "Lead-lag filter-based damping of virtual synchronous machines," *IEEE Trans. Ind. Appl.*, vol. 59, no. 6, pp. 6900–6913, 2023.